

MOEMS-based future systems for ELTs

Frederic Zamkotsian¹, Patrick Lanzoni¹, Rudy Barette¹, Michael Helmbrecht², Michael Feinberg³, Sébastien Lani⁴, Branislav Timotijevic⁴, Yves Petremand⁴

¹ Aix Marseille Univ, CNRS, CNES, LAM, Laboratoire d'Astrophysique de Marseille, 38 rue Frederic Joliot Curie, 13388 Marseille Cedex 13, France

² Iris AO, 2930 Shattuck Avenue, Berkeley, CA 94705, USA

³ Boston Micromachines Corporation, 30 Spinelli Place, Suite 103, Cambridge, MA 02138, USA

⁴ CSEM, Rue Jaquet-Droz 1, Neuchatel, CH-2002, Switzerland

e-mail: frederic.zamkotsian@lam.fr

ABSTRACT

MOEMS Deformable Mirrors (DM) are key components for next generation optical instruments implementing innovative adaptive optics systems, in existing telescopes as well as in the future ELTs. Due to the wide variety of applications, these DMs must perform at room temperature as well as in cryogenic and vacuum environment.

We tested the PTT 111 DM from Iris AO. The device could be operated successfully from ambient to 160 K; using our calibration procedure and a specific driving scheme, we obtained a quasi-identical best flat as low as 10nm rms at room temperature and 12nm rms at 160K.

We tested also Boston Micromachines segmented and continuous DMs at room temperature. Due to the accuracy and the repeatability of the electrostatic actuators, we were able to generate a synthetic influence function with a residual as low as 0.4% with respect to the actual influence functions measured for the whole actuation range.

We are engaged in a European development of tiltable micro-mirror arrays (MMA) exhibiting remarkable performances in terms of surface quality as well as ability to work at cryogenic temperatures. MMA with 100 x 200 μm^2 single-crystal silicon micromirrors were successfully designed, fabricated and tested down to 162 K. In order to fill large focal planes (mosaicing of several chips), we are currently developing large micromirror arrays to be integrated with their electronics. In future instrumentation, MOEMS DMs (wavefront correction) and tiltable MMAs (for object/field selection) are the key components for correcting/shaping the wavefront/field-of-view at the entrance or within the instruments. We propose new MOEMS-based instrument concepts in order to increase their efficiency and create new observational modes impossible to be implemented with current technologies. BATMAN family of spectro-imagers for current and future telescopes includes the MOEMS disruptive technology.

Keywords: MOEMS, micromirror array, cryogenic testing, adaptive optics, future generation spectro-imager.

1. MOEMS-BASED INSTRUMENTATION

1.1. MOEMS-based Adaptive Optics

Several research groups around the world are currently involved in the design of highly performing adaptive optical (AO) systems as well as for next generation instrumentation of 10m-class telescopes than for future extremely large optical telescopes. Wavefront correction like adaptive optics systems are based on a combination of three elements, the wavefront sensor for the measurement of the shape of the wavefront arriving in the telescope, the deformable mirror is the correcting element, and finally the real time computer closing the loop of the system at a frequency ranging from 0.5 to 3kHz, in order to follow the evolution of the atmospherical perturbations (Fig. 1).

Four main types of AO systems have been built or are under development: Single-Conjugate Adaptive Optics (SCAO), Multi-Conjugate Adaptive Optics (MCAO), Multi-Object Adaptive Optics (MOAO), and Extreme Adaptive Optics (ExAO). These AO systems are associated with different types of WaveFront Sensors (WFS), combined with natural guide stars or laser guide stars, and different architectures of Deformable Mirrors (DM). Numerous science cases will use these AO systems, SCAO, the "classical" AO system will provide accurate narrow field imagery and spectroscopy, MCAO, wide field imagery and spectroscopy, MOAO, distributed partial correction AO, and high dynamic range AO for

the detection and the study of circumstellar disks and extra-solar planets. Corrected fields will vary from few arcsec to several arcmin.

These systems require a large variety of deformable mirrors with very challenging parameters. For a 8m telescope, the number of actuators varies from a few 10 up to 5000; these numbers increase impressively for a 40m telescope, ranging from a few 100 to over 50 000, the inter-actuator spacing from less than 200 μm to 1 mm, and the deformable mirror size from 10 mm to a few 100 mm. Conventional technology cannot provide this wide range of deformable mirrors. The development of new technologies based on micro-opto-electro-mechanical systems (MOEMS) is promising for future deformable mirrors. The major advantages of the micro-deformable mirrors (MDM) are their compactness, scalability, and specific task customization using elementary building blocks. This technology permits the development of a complete generation of new mirrors. However this technology has also some limitation. For example, pupil diameter is an overall parameter and for a 40 m primary telescope, the internal pupil diameter cannot be reduced below 0.5 m. According to the maximal size of the wafers (8 inches), a deformable mirror based on MOEMS technology cannot be build into one piece. New AO architectures have been proposed to avoid this limitation.¹

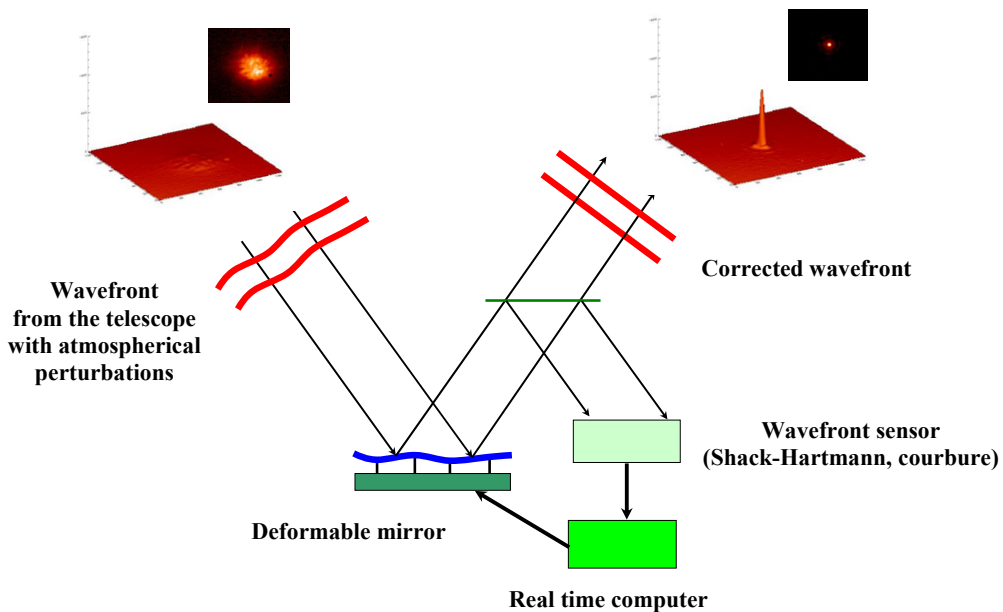


Fig. 1: Schematic of a wavefront correction system

LAM is involved since several years in conception of new MOEMS devices as well as in characterization of these components for the future instrumentation of ground-based and space telescopes. These studies include programmable slits for application in multi-object spectroscopy (JWST, European networks, EUCLID, BATMAN), deformable mirrors for adaptive optics, and programmable gratings for spectral tailoring.

1.2. MOEMS-based Spectro-Imager

LAM is leading the conception and realization of new MOEMS-based instruments. We are developing a 2048x1080 Digital-Micromirror-Device-based (DMD) MOS instrument to be mounted on the Telescopio Nazionale Galileo (TNG) and called BATMAN. A two-arm instrument has been designed for providing in parallel imaging and spectroscopic capabilities. BATMAN on sky is of prime importance for characterizing the actual performance of this new family of MOS instruments, as well as investigating new observational modes on astronomical objects, from faint and remote galaxies to active areas in nearby galaxies and small bodies of the solar system. This instrument will be placed at TNG by end-2020.²

BATMAN is a compact spectro-imager with two arms in parallel: a spectroscopic channel and an imaging channel. Both arms are fed by using the two DMD mirrors stable positions (Fig. 2).

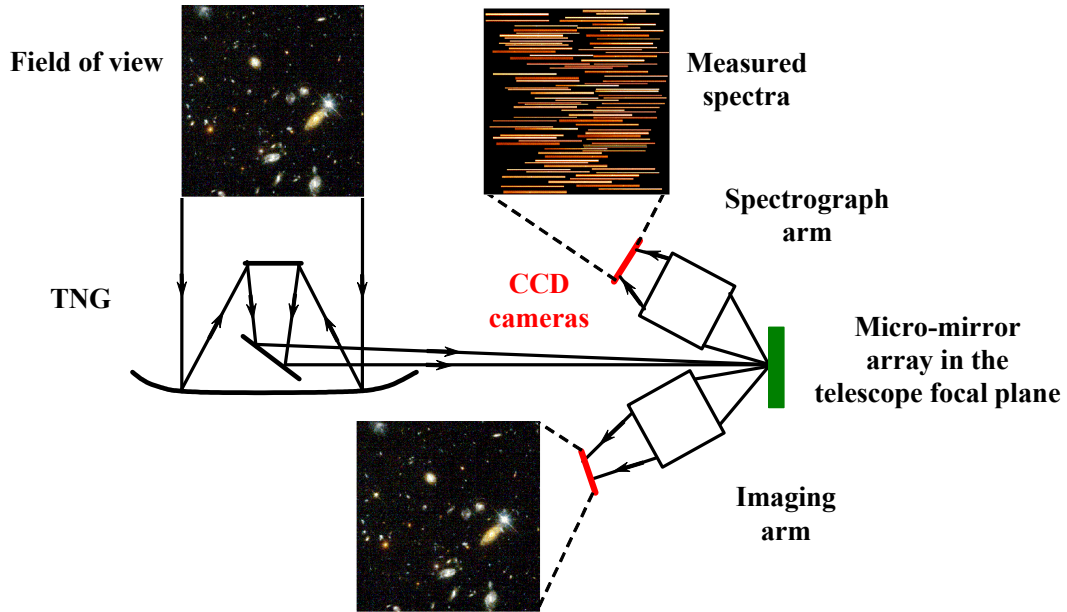


Fig. 2: Principle of BATMAN spectro-imager

Our goal is to make a robust and efficient instrument. Selecting a good starting point was really important. Previous works have been based onto smaller DMD chip areas and larger focal ratios, covering relatively smaller field of view. Here we concentrated to meet larger areas, still with simple optical layouts. In order to simplify as much as possible the optical layout of the system, we fixed some constraints:

- (a) focal ratios feeding DMD should be close to F/4, thus allowing relatively easy decoupling from the incoming and outgoing beams on the DMD surface;
- (b) incoming beam must hit DMD surface at normal incidence, everywhere on the DMD chip, translating into a simpler relay system not introducing tilted image planes and being telecentric;
- (c) both spectroscopy and imaging modes could be available, using the two ON/OFF state mode of micromirrors;
- (d) all optical components should lie in plane, for easy integration and alignment;
- (e) use as much as possible only plano and spherical optics, to reduce cost and delivery time.

Even if complex, we succeeded to design such a system, developing ideas proposed many years ago for the JWST near-infrared multi-object spectrograph.³ BATMAN baseline is resumed in Table 1.

Primary mirror diameter	3.6 m
Field of view	6.8 arcmin x 3.6 arcmin
Focal ratio	F/4 on DMD (with 2048 – 1080 micro-mirrors) Plate scale = 0.2 arcsec per micromirror
Beams on DMD	incoming light at normal incidence out-coming light at 24° DMD orientation at 45°
Wavelength range	400 - 800 nm
Spectral resolution	R=560 for 1 arcsec object (typical slit size)
Two arms instrument	one spectroscopic channel and one imaging channel
Detectors	Two 2k x 4k CCDs

Table 1: Baseline of BATMAN

Slit generator

Digital Micromirror Devices (DMD) from Texas Instruments could act as objects selection reconfigurable mask. The largest DMD chip developed by TI features 2048 x 1080 mirrors on a 13.68 μm pitch, where each mirror can be independently switched between an ON (+12°) position and an OFF (-12°) position. This component has been extensively studied in the framework of an ESA technical assessment of using this DMD component (2048 x 1080 mirrors) for space applications (for example in EUCLID mission). Specialized driving electronics and a cold temperature test set-up have been developed. Our tests reveal that the DMD remains fully operational at -40°C and in vacuum. A 1038 hours life test in space survey conditions (-40°C and vacuum) has been successfully completed. Total Ionizing Dose (TID) radiation tests, thermal cycling (over 500 cycles between room temperature and cold temperature, on a non-operating device) and vibration and shock tests have also been done; no degradation is observed from the optical measurements. **These results do not reveal any concerns regarding the ability of the DMD to meet environmental space requirements.**⁴

1.3. MOEMS Deformable Mirrors and programmable slits

Three main Micro-Deformable Mirrors (MDM) architectures are under study in different laboratories and companies. First, the bulk micro-machined continuous-membrane deformable mirror, studied by Delft University and OKO company, is a combination of bulk silicon micromachining with standard electronics technology⁵. This mirror is formed by a thin flexible conducting membrane, coated with a reflective material, and stretched over an electrostatic electrode structure. This mirror shows a very good mirror quality, but the mean deformed surface is a concave surface, and the number of actuators cannot be scalable to hundreds of electrodes. Second, the segmented, micro-electro-mechanical deformable mirror realized by Iris AO⁶ consists of a set of segmented piston-tip-tilt moving surfaces, fabricated in dense array. For adaptive optics application, the wavefront has to be properly sampled, increasing the number of actuators for a given number of modes to be corrected. Third, the surface micro-machined continuous-membrane deformable mirror made by Boston Micromachines Corporation (BMC) is based on a single compliant optical membrane supported by multiple attachments to an underlying array of surface-normal electrostatic actuators⁷. The efficiency of this device has been demonstrated recently in several AO system, including the GPI instrument on Gemini telescope. The third concept is certainly the most promising architecture, but it shows limited strokes for large driving voltages, and mirror surface quality may need further improvement for Extreme AO. All these devices are based on silicon or polysilicon materials.

We are particularly engaged in a European development of micromirror arrays (MMA) called MIRA for generating reflective slit masks in future Multi-object spectroscopy (MOS) instruments; this technique is a powerful tool for space and ground-based telescopes for the study of the formation and evolution of galaxies. MMA with 100 x 200 μm^2 single-crystal silicon micromirrors were successfully designed, fabricated and tested. Arrays are composed of 2048 micromirrors (32 x 64) with a peak-to-valley deformation less than 10 nm, a tilt angle of 24° for an actuation voltage of 130 V. The micromirrors were actuated successfully before, during and after cryogenic cooling, down to 162K. The micromirror surface deformation was measured at cryo and is below 30 nm peak-to-valley.^{8,9} In order to fill large focal planes (mosaicing of several chips), we are currently developing large micromirror arrays integrated with their electronics.

2. IRIS AO DEFORMABLE MIRROR

2.1. IRIS AO DM description

IRIS AO is producing segmented piston tip tilt mirrors with very flat mirrors. An exploded-view schematic diagram is presented in Fig. 3a. The DM array is paved by 37 hexagonal segments with a size of 700 μm from vertex-to-vertex, with a 606 μm pitch. The segment is capable of moving in piston/tip/tilt motions (PTT). In Fig. 3a, scaling is highly exaggerated in the vertical direction. In Fig. 3b is shown a die photograph of a 111-actuator 37-piston/tip/tilt-segment DM with 3.5 mm inscribed aperture (PTT111 device). The DM is manufactured using typical MEMS and integrated circuit materials such as polycrystalline silicon (polysilicon), silicon dioxides, silicon nitrides, and a proprietary bimorph material with similar coefficient of thermal expansion (CTE) to that of polysilicon. The s-shape of the bimorph flexures that elevates the DM segment is a result of engineered residual tensile stresses in the bimorph and actuator-platform polysilicon. After the DM is fabricated using highly stable MEMS materials, it is mounted onto a ceramic pin-grid array (PGA) package using an epoxy. The DM is sealed in nitrogen by epoxying a cover window over the DM.

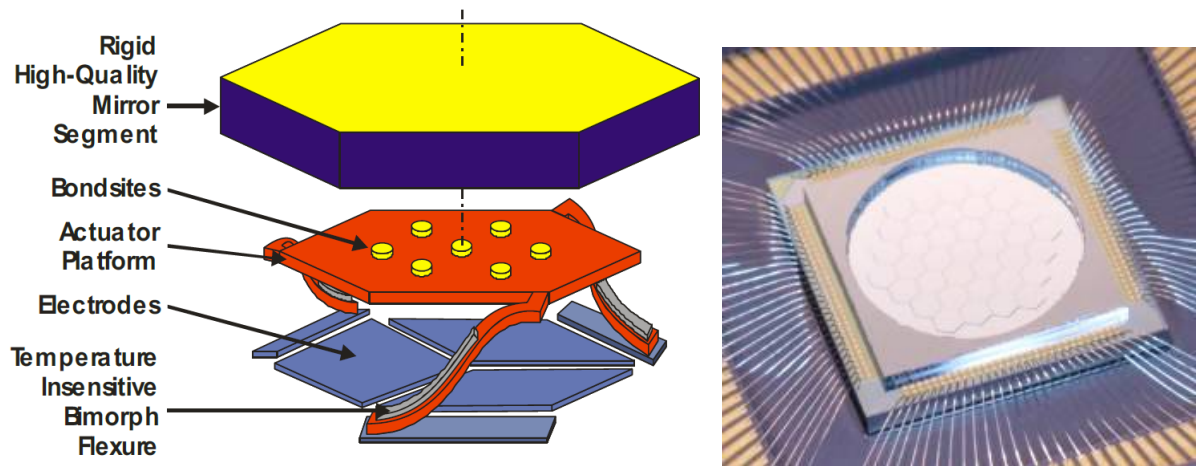


Fig. 3: Segmented MDM from Iris AO (a) Concept of one segment of the mirror;
 (b) Die photograph of a 111-actuator 37-piston/tip/tilt-segment DM with 3.5 mm inscribed aperture (PTT111 device)

To actuate the DM, the red actuator-platform layer is held at ground potential and the three diamond-shaped electrodes are energized at different electrical potentials. Applying the same voltage to all three electrodes pulls the segment in a piston motion toward the electrodes. A differential voltage across the electrodes results in tip and tilt motions. Because the positioning is highly repeatable, the DM segment motion can be calibrated, thus linearizing the DM position into orthogonal coordinates.

2.2. Cryogenic interferometric test set-up

The Laboratoire d'Astrophysique de Marseille has developed over the last few years an expertise in the characterization of micro-optical components. Our expertise in small-scale deformation characterization on the surface of micro-optical components has been conducted initially within the framework of the NASA study of a multi-object infrared spectrograph equipped with MOEMS-based slit masks for the JWST.

An interferometric characterization bench has been developed in order to measure the shape and the deformation parameters of these devices. All optical characterizations in static or dynamic behavior are performed, including measurements of optical surface quality at different scales, actuators stroke, maximum mirror deformation and cut-off frequency. This bench is a high-resolution and low-coherence Twyman-Green interferometer; out-of-plane measurement is performed with phase-shifting interferometry showing very high resolution (standard deviation <math>< 1\text{nm}</math>).¹⁰

Cryogenic characterization was carried out in a custom built cryogenic chamber installed in front of our interferometric setup. The cryo-chamber has a pressure as low as $10\text{e-}6$ mbar and is able to cool down to 100K, when not loaded, using a cryogenic generator.¹¹ The PTT111 device is packaged in PGA chip carrier and mounted in the cryo test set-up. The chamber is then closed by a flange and placed in front of the interferometer. Along the reference path, two compensation plates are placed for compensating the chamber window and the device window. By this way, we keep a high contrast for the interferometric fringes.

2.3. IRIS AO PTT111 surface characterization

Our experiment is done on an engineering grade device where the segments #23 and #24 are lockouts. The segment thickness is $25\mu\text{m}$ and the coating is protected silver. The maximum array stroke is $3.01\mu\text{m}$, and the maximum tilt angle is 5mrad. Fig. 4 is a picture of the device made on our bench (without the interferometric fringes). The two lockouts segments are at the upper right.

The device is driven either by the *Graphical User Interface* (GUI) provided by Iris-AO for the integration and pre-characterization phases. The interferometric measurements are done with the LAM-developed software, in Matlab, and linked with the Matlab driver provided by Iris AO. The GUI is showing a view of the mirror with numbered segments, and global Zernike coefficient as well as local (at segment level) Zernike coefficients could be tuned for each actuator/segment.¹²

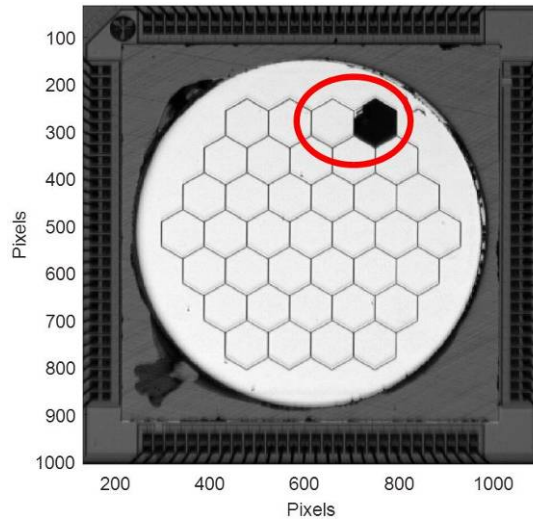


Fig. 4: PTT111 device tested in our experiment (engineering grade device)
Segments #23 and #24 (in the red circle) are lockouts.

We could then apply a serial of commands on the mirror. In Fig. 5, different mirror configurations are presented. From top left to bottom right, we can see:

- a pure piston (150nm) on the central M1 segment,
- a global astigmatism on the mirror, using the global Zernike coefficient set at 0.125
- a serial of three identical tilts on all segments in X direction, with 0.25mrad, 1.5mrad and 4.9mrad respectively.

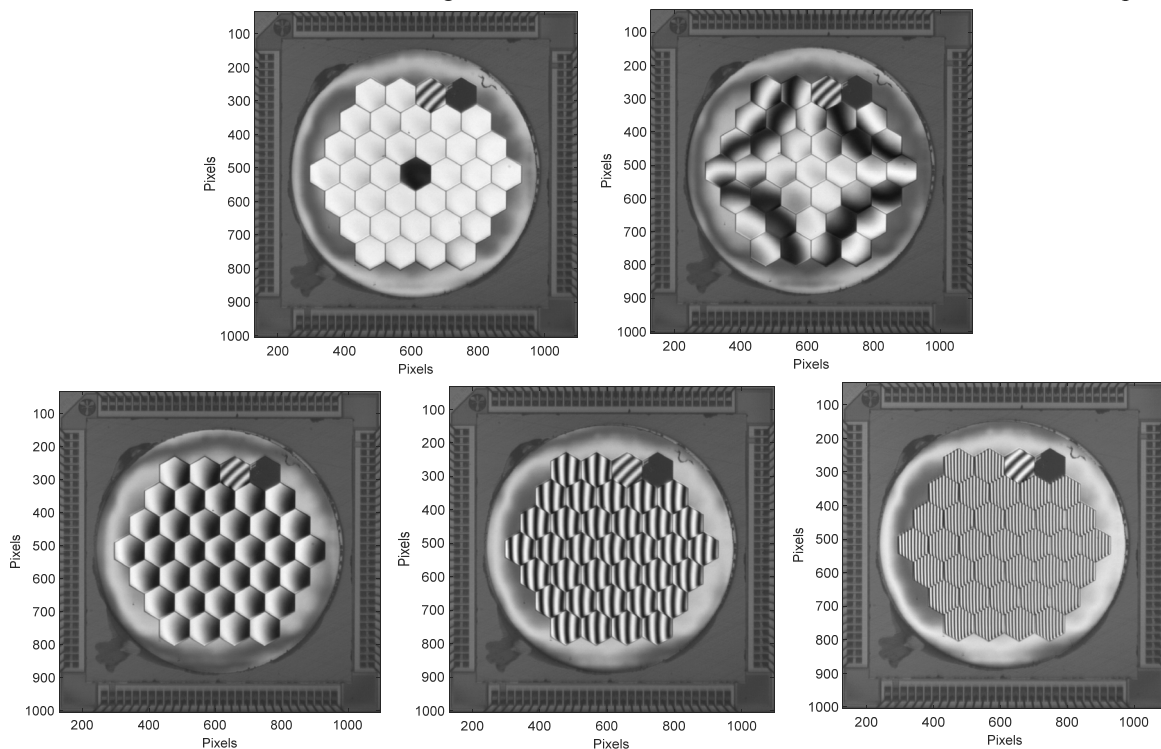


Fig. 5: top left: 150nm piston on segment#1; top right: astigmatism (0.125 on Zernike coefficient);
Bottom: Increasing tilt values along the X direction are applied to all segments (0.25, 1.5 and 4.9 mrad).

2.4. Best flat at ambient

Using the best flat provided by Iris AO, we obtained 17 nm RMS, 123 nm PtV surface deformation over the whole mirror. Note that this best flat is not corrected from the gravity effect occurring in our experiment, as the PTT111 is mounted in vertical position. In order to improve the best flat quality, we decided to develop an *improved best flat* procedure by measuring, with high accuracy, the tip-tilt and piston residuals and combining them with the original best flat values calibrated by Iris AO. We then obtain the improved best flat shown in Fig. 6.

The mirror surface deformation is then as low as 10 nm RMS, 79 nm PtV.

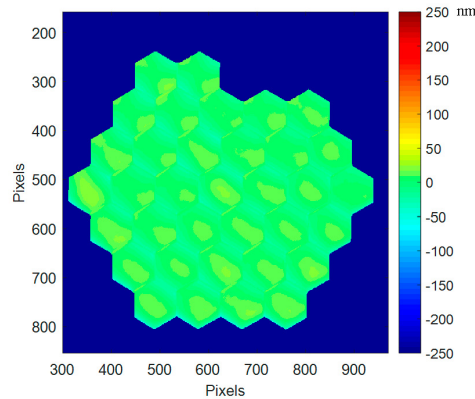


Fig. 6: Mirror surface deformation at ambient (293 K) when *improved best flat* condition is applied, after one cycle of cooling (10 nm RMS, 79 nm PtV)

Residual tilts with improved best flat are 6.5 μrad RMS (36 μrad PtV), while they were 32 μrad RMS (140 μrad PTV) with the original best flat. Residual pistons with improved best flat are 1.6 nm RMS (7 nm PtV), while they were 6.2 nm RMS (28 nm PtV) with the original best flat.¹²

This result shows the high quality of the mirror architecture and of the fabrication process. This flatness is a combination of a very good reproducibility of the actuator platform position after his elevation thanks to the bimorph flexures (Figure 3), and the choice of thick single-crystalline Silicon for the segment material. This position is very stable; long term measurement has been done at ambient on position stability and reproducibility, but this has not been done yet in cryo.

Improved best flat condition will be used in the following experiments.

2.5. Best flat at cryo

The device is then cooled down slowly from ambient temperature (293 K) down to 160 K, with the device constantly operating in its best flat condition. The PTT111 device is operating properly at all temperatures between 293 K and 160 K, and in vacuum.

Every 10 K an interferometric measurement is done in order to follow the differential deformation of the mirror at whole mirror level as well as at segment level. Several patterns are applied and measured in order to see the ability of the device to behave as at room temperature; the applied “patterns” are best flat, pure pistons on some segments, and different tilts on the segments. Due to the vibrations induced by the cryo pump on the sample, we have to stop it during the measurement, leading to a limited increase of the temperature during the measurement duration. Phase shifting interferometry parameters have been adjusted in order to minimize the measurement time to a few minutes.

In Figure 7, the best flat surface deformation at cryo (160 K) is given with the best flat condition as calibrated at ambient. A global convex deformation is observed reaching a deformation of 86 nm RMS, 501 nm PtV. Some additional deformations (mainly tilts) are observed on some segments at the upper left side (segments #26, 27, and 28). The global convex shape in cryo is due to the packaging “shrinking” in cryo. The Coefficient of Thermal Expansion (CTE) mismatch between die/package materials induces a global effect on the mirror when cooled down at 160 K. The mirror is operating perfectly in cryo, and a “new” best flat condition will be developed and described in the next paragraphs.

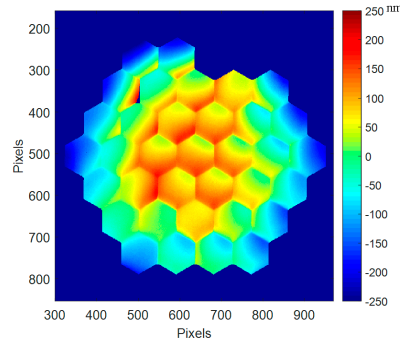


Fig. 7: Best flat mirror deformation at cryo (160 K), first run, with the original best flat calibrated at ambient (86 nm RMS, 501 nm PtV).

We measure and sort out for each segment tilt and piston values: the tilts have a value of 200 μrad RMS (950 μrad PtV) while the pistons expands on 74 nm RMS (239 nm PtV). Tilts and pistons are not behaving the same way. Pistons are behaving within the three concentric rings of PTT111 37 segments, with a common motion for the central area (segments #1 to 7), the middle ring (segments #8 to 19), and the outer ring (segments #20 to 37); residual pistons at are 6.2 nm RMS (28 nm PtV), and 74 nm RMS (239 nm PTV) in cryo; this effect is clearly related to the shrinkage of the overall device. As for the tilts, they don't show a clear pattern; they are scattered away from the original positions at ambient: residual tilts at ambient are 32 μrad RMS (140 μrad PtV), and 200 μrad RMS (950 μrad PTV) in cryo; this differential evolution is possibly due to the different modification of the complex structure underneath each segment: the actuator platform, the bonding pads, the mirror segment, the coating, and the underlying 3 legs bimorph structure.

In order to demonstrate full operation of PTT111 at cryogenic temperature, we decide to cool down the device and optimize in-situ all actuators for generating a cryo best flat. Our strategy is a weighted addition of the consecutive measurement residual errors and, using Iris AO electronics, we are loading these calculated values actuator by actuator, departing from the original values provided by Iris AO, and applying them to the device. Our *cryo best flat* condition is a combination of [best flat calibrated by Iris-AO at ambient, improved best flat at ambient, improved best flat in cryo (first run), improved best flat in cryo (second run)]. **Then, in a single measurement step and applying this best flat condition, we got, at 160 K, a mirror surface deformation as low as 12 nm RMS, 113 nm PtV** (Figure 8).

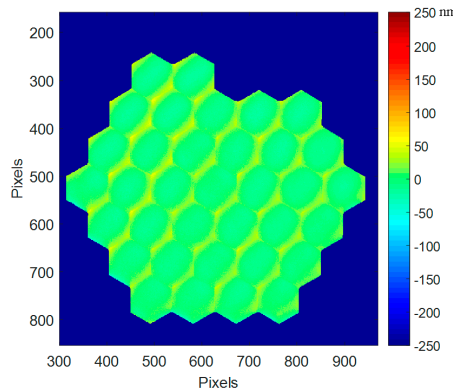


Fig. 8: Mirror surface deformation at cryo (160 K), second run, when *cryo best flat* condition is applied (12 nm RMS, 113 nm PtV);

Our *cryo best flat* at 160 K is then very close to our *improved best flat* at ambient (293 K), showing our ability to operate properly PTT111 device in cryo. The deformation difference is 2 nm RMS, 34 nm PtV between 160 K and 293 K. This additional deformation is due mainly to the mirror segment deformation, as revealed in the following paragraph 2.6.

Residual tilts with *cryo best flat* are 3.5 μrad RMS (17 μrad PtV), while they were 6.5 μrad RMS (36 μrad PtV) with the *improved best flat* at ambient. Residual pistons with *cryo best flat* are 1.2 nm rms (4.3 nm PtV), while they were 1.6 nm RMS (7 nm PtV) with the *improved best flat* at ambient.

A second loop of best flat optimisation is useless as the remaining mirror surface deformation is only due to the contributions of individual segment deformations. As the additional deformation of PTT111 at cryo is 501 nm PtV, the *cryo best flat* is compensating this deformation, minimizing the whole mirror deformation, down to 12 nm RMS (123 nm PtV). Then, as the maximum stroke of this device is originally 3.01 μm at ambient, the operational stroke is reduced to 2.5 μm at cryo (16.7% stroke reduction).

2.6. Segment characterization

Thanks to our set-up spatial resolution, we have several thousand measurement points per segment. It is then possible to measure, at segment level, the deformation induced by the strong temperature change from ambient to cryo. The surface deformation by segments at ambient has a mean value of 7.2 nm with a standard deviation of 1.5 nm, and at 160 K, a mean value of 8.5 nm with a standard deviation of 1.6 nm. By selecting a typical segment, a closer analysis of the segment evolution at cryogenic temperature could be done, especially on its shape. We could show clearly that the convex cylindrical shape at ambient is changing to an astigmatic concave shape at cryo. At ambient (293 K), the segment surface deformation is 5 nm RMS (24 nm PtV), while at 160 K the deformation is still low, at 8 nm RMS (47 nm PtV). The deformation difference between ambient and 160 K reveals a pure concave axisymmetrical change of 4.9 nm RMS (71 nm PtV). This is due to the CTE mismatch between the single-crystalline silicon and the silver-protected coating deposited on top of the segment. All segments are behaving in the same way; the mean deformation at ambient is in the range of 25 nm, while it rises to 50 nm in cryo. This deformation difference is still within the requirement of almost all foreseen wavefront correction systems. This deformation difference at segment level is the major contribution to the whole mirror surface deformation.

3. BOSTON MICROMACHINES DEFORMABLE MIRROR

3.1. BMC Deformable Mirror

BMC produces the most advanced MEMS deformable mirrors. The concept is based on an array of electrostatic actuators linked one by one to a continuous top mirror (Fig. 9). Their main parameters are approaching the requirements values, i.e. large number of actuators (up to 4096, see Fig. 9), large stroke (up to 5.5 μm), good surface quality, but they still need large voltages for their actuation (150–250V).

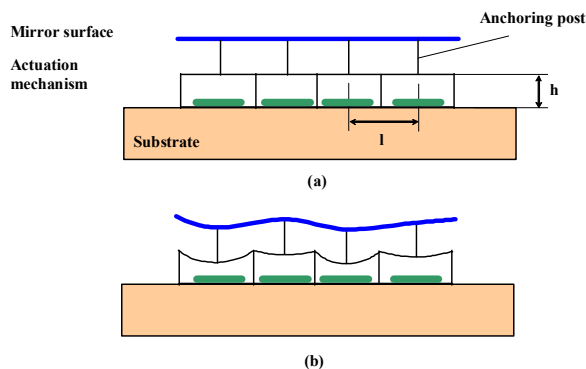


Fig. 9: Continuous membrane MDM from BMC

3.2. BMC DM surface characterization

We tested a Boston Micromachines DM of 32x32 actuators on a square array, with 1020 active actuators. The inter-actuator pitch is 300 μm , for a total size of the DM 9.3 mm. Boston Micromachines announces a subnanometric minimum stroke and a total stroke of 1.5 μm . A picture of the device installed in front of our measurement set-up is shown in Fig. 10a.

The bench developed at LAM is a high-resolution and low-coherence Twyman-Green interferometer; with phase-shifting measurement technique, showing very high resolution (standard deviation < 1nm).¹⁰ Two fields of view are easily accessible in our set-up: a large field of view able to image the full DM aperture and a small field of view for imaging few actuators on the surface. A close-up view of the mirror surface is given in Fig 10b with 7x6 actuators, revealing the

attachment posts traces as well as the release holes placed all over the surface (holes allowing the removal of the sacrificial layers in the MOEMS DM process).

At first, we applied the same voltage of 70% (with respect to the maximal voltage allowed by the manufacturer) to all the actuators. The first observation is that a uniform voltage on all the actuators does not correspond to a flat surface on the DM (Fig. 10c). The general shape is a defocus over the entire surface of approximately 500 nm peak-to-valley; note the actuator #769 (bottom left), which is fixed to 0%. When a uniform voltage of 90% is applied, the same behavior is observed. By removing the defocus, a surface deformation of 32nm is measured. Measurement on the small field of view shows that, at actuator level, most of the deformation is linked to the holes and post traces and their vicinities.¹³ We have measured a maximum stroke of 1.1 μ m, slightly less than the value indicated by Boston Micromachines.

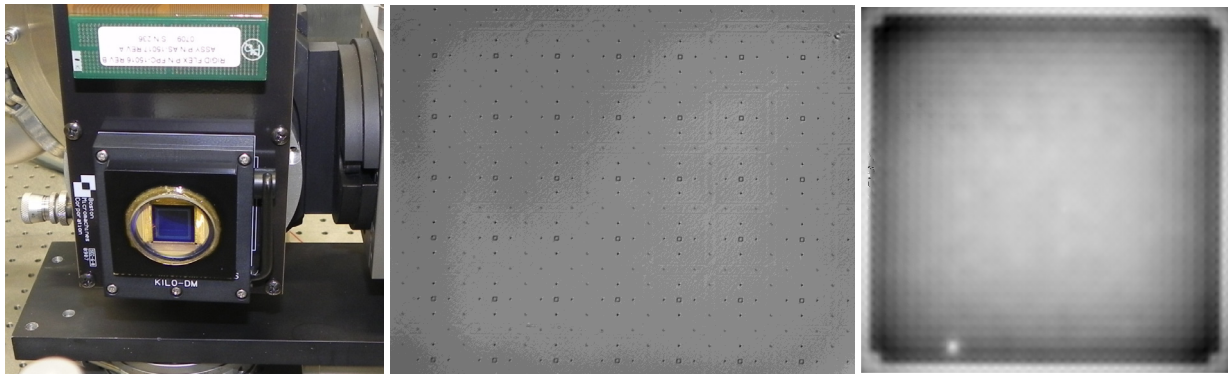


Fig. 10: (a) Boston Micromachines DM mounted on the interferometric bench; (b) Close-up view of some actuators of the DM; (c) Interferometric measurement of the entire DM (one actuator is not operating)

The measurement of the influence function has been made for all actuators. A detailed study has been done on one of the central actuators (actuator #272): all actuators on the DM are set to 50% voltage and voltage of the actuator #272 is varied from 0% (convex shape) to 100% (concave shape) with more fine voltage tuning at high values; this is done in order to precisely characterize the behavior of the actuator, taking into account the quadratic nature of the electrostatic force. In Fig. 11a, the fringe pattern is shown for a 800nm deformation: there is a slight non rotational symmetry. The central part of the influence function is almost a Gaussian, but do not take into account the wings.¹³ In Fig. 11b is given the profile of the deformed surface when the voltage is varied from 0% to 100%. The profiles are not symmetric vertically, due to quadratic electrostatic force: for a higher voltage, the gap in the actuator is smaller leading to a larger force than for a lower voltage. The positions of the tips of the influence functions are given in Fig. 11c, revealing clearly the quadratic electrostatic force.

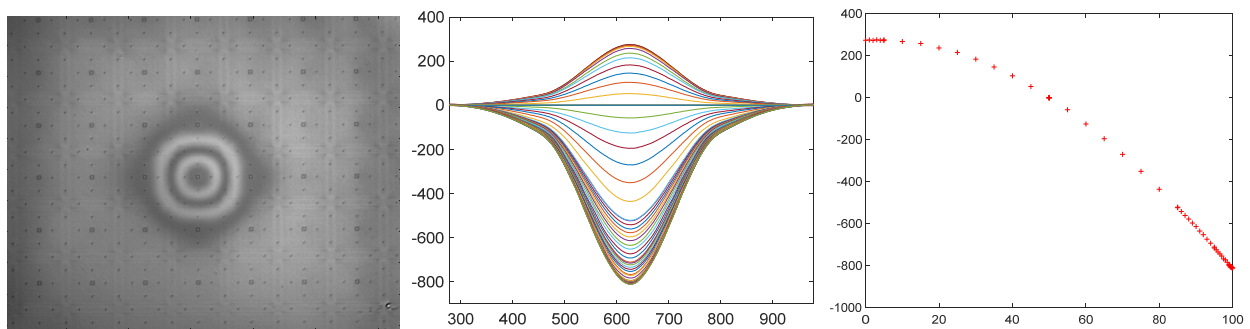


Fig. 11: (a) Interferometric fringes when the central actuator #272 is actuated;
 (b) Influence function with 50% voltage on all actuators, 0%-100% voltage on the tested actuator;
 (c) Actuator tip displacement with respect to the voltage percentage.

From all actual influence functions, a synthetic influence function has been generated and is shown in Fig. 12 with its overall shape as well as with one profile. **The global departure for all actual influence functions to the synthetic influence function is below 0.4% rms.**

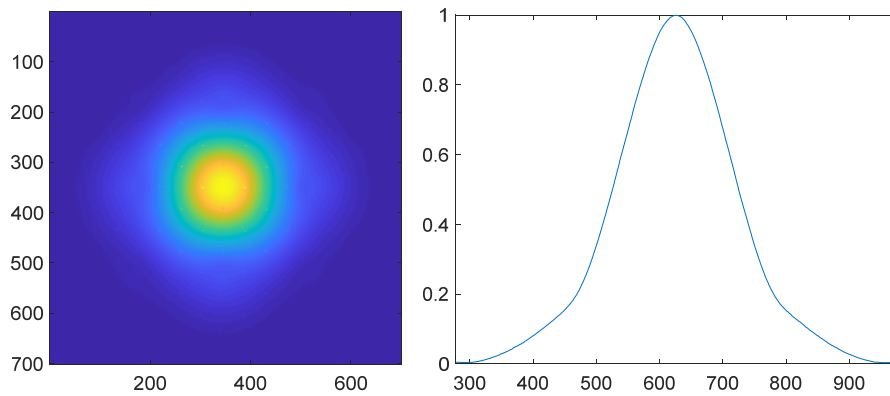


Fig. 12: (a) Synthetic influence function;
(b) Profile of the synthetic influence function.

4. MIRA: A EUROPEAN TILTABLE MICRO-MIRROR ARRAY

In future space missions for Universe and Earth Observation, scientific return could be optimized using MOEMS devices. Large micromirror arrays (MMA) are used for designing new generation of instruments. In Universe Observation, multi-object spectrographs (MOS) are powerful tools for space and ground-based telescopes for the study of the formation and evolution of galaxies. This technique requires a programmable slit mask for astronomical object selection; 2D micromirror arrays are perfectly suited for this task. In Earth Observation, removing dynamically the straylight at the entrance of spectrographs could be obtained by using a Smart Slit, composed of a 1D micro-mirror array as a gating device.

We are currently engaged in a European development of micro-mirror arrays, called MIRA, exhibiting remarkable performances in terms of surface quality as well as ability to work at cryogenic temperatures. MMA with $100 \times 200 \mu\text{m}^2$ single-crystal silicon micromirrors were successfully designed, fabricated and tested down to 162 K. In order to fill large focal planes (mosaicing of several chips), we are currently developing large micromirror arrays to be integrated with their electronics (Fig.13). 1D and 2D arrays are built on wafer with Through Wafer Vias in order to allow routing of the device on wafer backside, foreseeing integration with dedicated ASICs. The yield of these devices as well as contrast enhancement have been successfully implemented.¹⁴

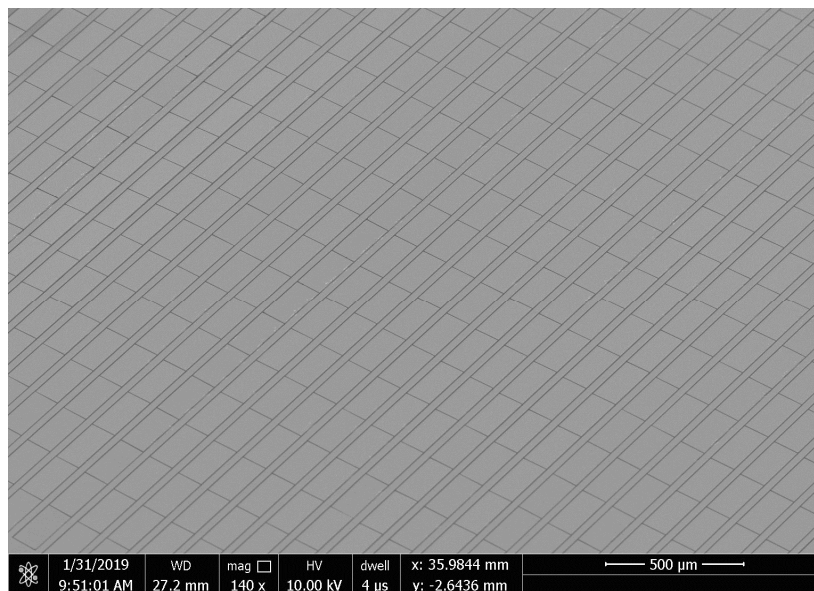


Fig. 13: 64 x 32 micromirror array with high fill factor in the vertical direction providing long slits. Each mirror measures $200 \times 100 \mu\text{m}^2$. Wafer level bonding steps are required to process these arrays.

5. CONCLUSION

MOEMS Deformable Mirrors and MOEMS tiltable micro-mirror arrays are key components for next generation optical instruments implementing innovative instrumentation, in existing telescopes as well as in the future ELTs. Due to the wide variety of applications, these MOEMS components must perform at room temperature as well as in cryogenic and vacuum environment. The PTT 111 DM from Iris AO has been operating successfully from ambient to 160 K; using our calibration procedure and a specific driving scheme, with a quasi-identical best flat as low as 10nm rms at room temperature and 12nm rms at 160K. The Boston Micromachines kilo-DM has been tested at room temperature and a synthetic influence function has been obtained from the measurements with a residual as low as 0.4%. MIRA device, our European tiltable micro-mirror array, is exhibiting remarkable performances in terms of surface quality as well as ability to work at cryogenic temperatures, down to 162 K. In order to fill large focal planes (mosaicing of several chips), we are currently developing large micromirror arrays to be integrated with their electronics.

In future instrumentation, MOEMS DMs (wavefront correction) and tiltable MMAs (for object/field selection) are the key components for correcting/shaping the wavefront/field-of-view at the entrance or within the instruments. We propose new MOEMS-based instrument concepts in order to increase their efficiency and create new observational modes impossible to be implemented with current technologies. BATMAN family of spectro-imagers for current and future telescopes includes the MOEMS disruptive technology.

REFERENCES

- [1] F. Zamkotsian, K. Dohlen, "Prospects for MOEMS-based adaptive optical systems on extremely large telescopes", in *Proceedings of the conference Beyond conventional Adaptive Optics*, Venice, Italy (2001)
- [2] Frederic Zamkotsian, Patrick Lanzoni, Nicolas Tchoubaklian, Harald Ramarijaona, Manuele Moschetti, Marco Riva, Marc Jaquet, Paolo Spano, William Bon, Mathieu Vachey, Luciano Nicastro, Emilio Molinari, Rosario Cosentino, Adriano Ghedina, Manuel Gonzalez, Walter Boschini, Paolo Di Marcantonio, Igor Coretti, Roberto Cirami, Filippo Zerbi, Luca Valenziano, "BATMAN @ TNG: Instrument integration and performance", in *Proceedings of the SPIE conference on Astronomical Instrumentation 2018*, Proc. SPIE **10702**, Austin, USA, (2018)
- [3] F. Zamkotsian, K. Dohlen, D. Burgarella, V. Buat, "Aspects of MMA for MOS: optical modeling and surface characterization, spectrograph optical design", in *Proceedings of the NASA conference on "NGST Science and Technology Exposition"*, ASP Conf. Ser. **207**, 218-224, Hyannis, USA, (1999)
- [4] F. Zamkotsian, P. Lanzoni, E. Grassi, R. Barette, C. Fabron, K. Tangen, L. Valenziano, L. Marchand, L. Duvet "Successful evaluation for space applications of the 2048x1080 DMD," in *Proceedings of the SPIE conference on MOEMS 2011*, Proc. SPIE **7932**, San Francisco, USA (2011)
- [5] G. Vdovin, S. Middelhoek and P. M. Sarro, "Technology and applications of micromachined silicon adaptive mirrors", *Opt. Eng.*, **36** (5), 1382-1390 (1997)
- [6] M.A. Helmbrecht, M. He, C.J. Kempf, F. Marchis "Long-term stability and temperature variability of Iris AO segmented MEMS deformable mirrors", Proc. SPIE **9909**, (2016)
- [7] S. Cornelissen, T. G. Bifano "Advances in MEMS deformable mirror development for astronomical adaptive optics", in *Proceedings of the SPIE conference on MOEMS 2012*, Proc. SPIE **8253**, San Francisco, USA (2012)
- [8] S. Waldis, F. Zamkotsian, P.-A. Clerc, W. Noell, M. Zickar, N. De Rooij, "Arrays of high tilt-angle micromirrors for multiobject spectroscopy," *IEEE Journal of Selected Topics in Quantum Electronics* **13**, pp. 168–176 (2007).
- [9] M. Canonica, F. Zamkotsian, P. Lanzoni, W. Noell, N. de Rooij, "The two-dimensional array of 2048 tilting micromirrors for astronomical spectroscopy," *Journal of Micromechanics and Microengineering*, 23 055009, (2013)
- [10] A. Liotard, F. Zamkotsian, "Static and dynamic micro-deformable mirror characterization by phase-shifting and time-averaged interferometry", in *Proceedings of the SPIE conference on Astronomical Telescopes and Instrumentation 2004*, Proc. SPIE **5494**, Glasgow, United Kingdom (2004)
- [11] F. Zamkotsian, E. Grassi, S. Waldis, R. Barette, P. Lanzoni, C. Fabron, W. Noell, N. de Rooij, " Interferometric characterization of MOEMS devices in cryogenic environment for astronomical instrumentation," Proc. SPIE **6884**, San Jose, USA, (2008)
- [12] F. Zamkotsian, , P. Lanzoni, R. Barette, M. Helmbrecht, F. Marchis, A. Teichman, " Operation of a MOEMS Deformable Mirror in Cryo: Challenges and Results," *Micromachines* **8**, 233; doi:10.3390/mi8080233 (2017)
- [13] Johan Mazoyer, Raphael Galicher, Pierre Baudoz, Patrick Lanzoni, Frédéric Zamkotsian, Gérard Rousset, "Deformable mirror interferometric analysis for the direct imagery of exoplanets" in *Proceedings of the SPIE conference on Astronomical Instrumentation 2014*, Proc. SPIE **9148**, Montréal, Canada, (2014)
- [14] Frederic Zamkotsian, Yves Petremand, Patrick Lanzoni, Sébastien Lani, Rudy Barette, Branislav Timotijevic, Michel Despont, "Large 1D and 2D micro-mirror arrays for Universe and Earth Observation", *Proceedings of the SPIE conference on MOEMS 2019*, Proc. SPIE **10931**, San Francisco, USA, (2019)